Second-Order Model of Membrane Electric Field Induced by Alternating External Electric Fields

Tadej Kotnik and Damijan Miklavčič

Faculty of Electrical Engineering, University of Ljubljana, SI-1000 Ljubljana, Slovenia

Second-Order Model of Membrane Electric Field Induced by Alternating External Electric Fields

Tadej Kotnik* and Damijan Miklavčič

Abstract—**With biological cells exposed to ac electric fields below 100 kHz, external field is amplified in the cell membrane by a factor of several thousands (low-frequency plateau), while above 100 kHz, this amplification gradually decreases with frequency. Below 10 MHz, this situation is well described by the established first-order theory which treats the cytoplasm and the external medium as pure conductors. At higher frequencies, capacitive properties of the cytoplasm and the external medium become increasingly important and thus must be accounted for. This leads to a broader, second-order model, which is treated in detail in this paper. Unlike the first-order model, this model shows that above 10 MHz, the membrane field amplification stops decreasing and levels off again in the range of tens (high-frequency plateau). Existence of the high-frequency plateau could have an important impact on present theories of high-frequency electric fields effects on cells and their membranes.**

Index Terms—**AC electric fields, electric field stimulation, membrane electric field, membrane electrodynamics, transmembrane voltage.**

I. INTRODUCTION

EXPOSURE of biological cells to electric fields can lead to a variety of biophysical and biochemical responses. Applications based on these responses can roughly be divided into two groups. The first group uses electric fields as a tool to modify various properties of the cells. Herein are the applications that utilize the increase in membrane permeability caused by electric fields for introduction of various molecules into cells [1]–[3], insertion of molecules into cell membranes [4], [5], and fusion of cells [6], [7]. The second group of applications uses electric fields and currents as tools to characterize various properties of biological cells or their constituents, both in suspensions and in tissues. Among the most important approaches in such characterization is the evaluation of cell's response to electric fields at different frequencies. By varying the frequency of the field, values of the measured parameters form spectra: frequency dependence of bulk dielectric permittivity of a suspension or tissue constitutes its dielectric relaxation spectrum [8], frequency dependence of the cellular angular velocity in rotating electric fields forms the electrorotational spectrum [9], and frequency dependence of the cellular translational velocity in nonuniform alternating fields is the dielectrophoretic spectrum [10]. With these methods, various physical quantities can be determined that are difficult to assess by direct measurement (e.g., conductivity and capacitance of the membrane and the cytoplasm).

The basic mechanism underlying majority of these methods is the inducement of potential difference across the membrane by the external electric field, which results in the transmembrane voltage (TMV) and membrane electric field. When induced by ac fields, these quantities depend on frequency, and the knowledge of this dependence is of significant importance for the understanding of more complex phenomena, such as the spectra mentioned above.

The classical theory of transmembrane voltage inducement has been developed in the 1950's by H. P. Schwan and co-workers [11], [12]. In this theory, both the cytoplasm and the extracellular medium are described as purely conductive (i.e., having nonzero conductivity, but zero dielectric permittivity), while the membrane is treated as a lossy dielectric (i.e., having both nonzero conductivity and permittivity). This leads to the description of the inducement as a first-order process characterized by a time constant [12]

$$\tau_m = \frac{Rc_m}{\frac{2\lambda_i\lambda_e}{\lambda_i+2\lambda_e} + \frac{R}{d}\lambda_m} \tag{1}$$

where λ_i, λ_m, and λ_e are the conductivities of the cytoplasm, cell membrane, and extracellular medium, respectively, R is the cell radius, d is the membrane thickness, and $c_m = \varepsilon_m/d$ is the membrane capacitance, with ε_m denoting the dielectric permittivity of the membrane.[1]

This description also allows for the derivation of the TMV induced by an external ac electric field. Written in the frequency plane, it reads [13]

$$U_m(\omega, \theta) = \frac{3}{2}E_e R \cos\theta \frac{1}{1 + j\omega\tau_m} \tag{2}$$

where E_e is the amplitude of the external electric field, θ is the polar angle measured with respect to the direction of the field, and $\omega = 2\pi f$, with f denoting the frequency of the field. In (2), U_m is complex; its absolute value gives the amplitude of the TMV, while its argument is the directed angle corresponding to the phase shift between U_m and E_e (a negative value implies a lag of U_m behind E_e).

[1]We use the term "permittivity" for the total permittivity of the material, i.e., the product of the relative permittivity of the material (e.g., $\varepsilon_{r\,\text{water},20°C} \approx 80.3$) and the dielectric constant of the vacuum ($\varepsilon_0 = 8.854 \times 10^{-12}$ As/Vm).

TABLE I
VALUES USED IN THE CALCULATIONS

Parameter	Symbol	Value	Reference
Cell radius	R	10 μm	
Membrane thickness	d	5 nm	[29]
Conductivity of the cytoplasm	λ_i	0.3 S/m	[30], [31]
Conductivity of the membrane	λ_m	3×10^{-7} S/m	[32]
Conductivity of the extracell. medium	λ_e	1.2 S/m	[33] (blood serum at 35°C)
Permittivity of the cytoplasm	ε_i	6.4×10^{-10} As/Vm	set at the same value as ε_e
Permittivity of the membrane	ε_m	4.4×10^{-11} As/Vm	[32]
Permittivity of the extracell. medium	ε_e	6.4×10^{-10} As/Vm	[17], [34] (physiological saline at 35°C)

We choose for the sake of clarity to henceforth treat the conditions at $\theta = 0$, where U_m has a peak value. We denote $U_m(\omega) \equiv U_m(\omega, 0)$ and (2) becomes

$$U_m(\omega) = \frac{3}{2} E_e R \frac{1}{1 + j\omega\tau_m} \qquad (3)$$

while the spatial dependence on θ is restored by simply multiplying the result by $\cos\theta$ (this also applies to E_m and G_E, which will be introduced in the following paragraphs).

Throughout the derivation of the TMV, cell membrane is assumed to be homogeneous. Retaining this assumption, the induced membrane electric field can be calculated as

$$E_m(\omega) = \frac{U_m(\omega)}{d} \qquad (4)$$

and the amplification of the external electric field in the membrane is then given by

$$G_E(\omega) = \frac{E_m(\omega)}{E_e} = \frac{3R}{2d} \frac{1}{1 + j\omega\tau_m}. \qquad (5)$$

If typical values are assigned to the parameters contained in (1) and (5) (Table I), the magnitude of the amplification $|G_E(\omega)|$ (i.e., the ratio of the amplitudes of E_m and E_e) and the phase $\angle G_E(\omega)$ (i.e., the phase shift between E_m and E_e) can be plotted as functions of frequency in form of a Bode plot (Fig. 1).

According to (5), far below the *breakpoint frequency* $f = 1/(2\pi\tau_m)$, which is approximately 100 kHz in physiological conditions (Table I), the amplification is practically constant (the *low-frequency plateau*). Above the breakpoint frequency, $|G_E(\omega)|$ is decreasing, asymptotically approaching a negative unit slope. The limiting values at $\omega \to 0$ and $\omega \to \infty$ are easily determined

$$|G_E(0)| = \frac{3R}{2d}, \quad \angle G_E(0) = 0° \qquad (6)$$

$$|G_E(\infty)| = 0, \quad \angle G_E(\infty) = -90°. \qquad (7)$$

While the situation at low frequencies is not significantly affected by the assumption of purely conductive properties of the cytoplasm and extracellular medium, it becomes progressively
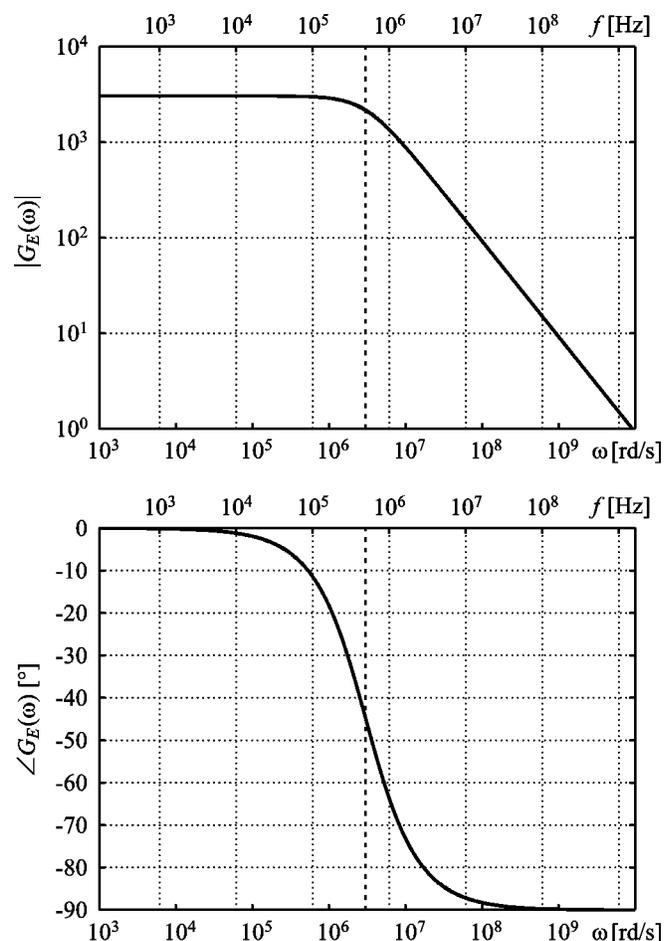

Fig. 1. Bode plot of the amplification of an external ac electric field in the membrane according to the established first-order treatment given by (5). Top: magnitude of the amplification; bottom: phase of the amplification (negative phase corresponds to a lag of the membrane field behind the external field). In each graph, the bottom abscissa gives the angular frequency $\omega = 2\pi f$, and the top abscissa gives the corresponding frequency f. The bold dotted vertical corresponds to the breakpoint frequency $f = 1/2\pi\tau_m$. Parameter values used in the calculation are given in Table I.

more questionable with increase in frequency, as the capacitive properties of both the cytoplasm and the extracellular medium gain importance. In this paper, we reevaluate the process of TMV and membrane field inducement in ac electric fields, with
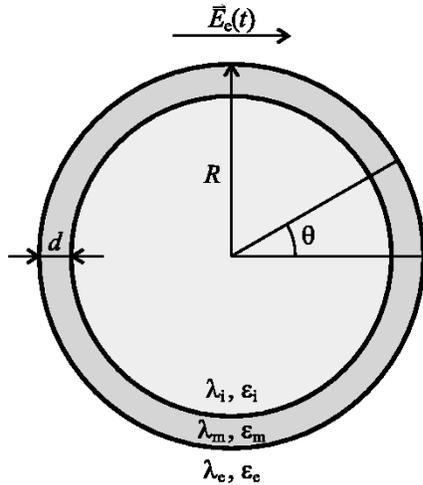
Fig. 2. In the model on which our calculations are based, the cell is a sphere with radius of R, enclosed by a membrane of uniform thickness d. External electric field is homogeneous and retains its orientation, but its strength E_e varies with time. Conductivities and permittivities are attributed to regions occupied by cytoplasm $(\lambda_i, \varepsilon_i)$, membrane $(\lambda_m, \varepsilon_m)$ and extracellular medium $(\lambda_e, \varepsilon_e)$.

each of the regions assigned both a nonzero electric conductivity and dielectric permittivity. We show that in the submegahetz range, predictions of the derived model are very close to (5), but then start to diverge, quickly leading to significant differences between the two models.[2]

II. METHOD OF ANALYSIS

A spherical cell surrounded by a medium represents a system characterized by two geometrical parameters, namely cell radius (R) and membrane thickness (d), and three sets of material parameters, each describing the properties of an individual material within the system (the cytoplasm, cell membrane, and extracellular medium). If the system is exposed to electric fields, the set of parameters describing a material consists of two quantities—its electric conductivity (λ) and dielectric permittivity (ε). This model is depicted in Fig. 2.

Though treatment of materials as pure conductors is under some circumstances justified, in reality every material demonstrates some dielectric permittivity, which affects the electric field propagation and, more importantly, subsequent electric field redistribution due to polarization effects. To enable a treatment similar to that of pure conductors, conductivity and

[2]Equation (5) is also invalid when cells are suspended in an artificial medium with a conductivity several orders of magnitude lower than physiological [12]. While this paper focuses on the physiological environment, the process of inducement in general media is treated in detail in [15].
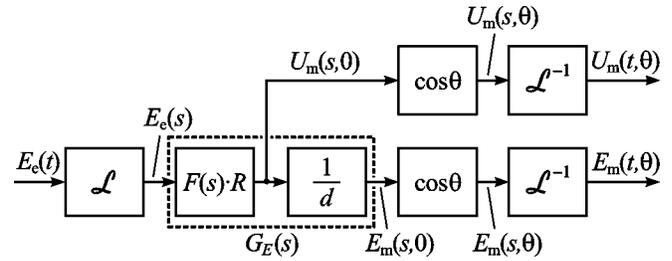

Fig. 3. To determine the time courses of transmembrane voltage and membrane electric field induced by a time-varying external electric field, the time course of the external field must first be described in terms of a function $E_e(t)$. The Laplace transform then gives the corresponding $E_e(s)$. The product of $E_e(s)$, $F(s)$, R and $\cos\theta$ represents the induced transmembrane voltage in complex-frequency space, $U_m(s)$, while an additional division by d gives the induced membrane field, $E_m(s)$. The inverse Laplace transform casts both results into the time domain. Due to the linearity of the system, the blocks of the system can be distributed in several equivalent ways, with this particular arrangement showing $G_E(s)$ as a compact subsystem.

permittivity of the material are combined into the *admittivity operator* [14]

$$\{\lambda, \varepsilon\} \to \Lambda = \lambda + \varepsilon \frac{\partial}{\partial t} \qquad (8)$$

To avoid the use of differential operators, the analysis is transferred from the time domain into the complex-frequency domain, where Λ becomes

$$\Lambda = \lambda + \varepsilon s \qquad (9)$$

with s denoting the complex frequency.

Replacement of the differential terms with pure algebraic expressions considerably simplifies the analysis and thus allows for treatment of structured systems consisting of several materials, such as the system in Fig. 2. Pursuing this approach, the induced transmembrane voltage is given by [14]

$$U_m(s, \theta) = F(s)E_e(s)R\cos\theta \qquad (10a)$$

where $E_e(s)$ is the Laplace (Heaviside) transform of the time course of the electric field strength $E_e(t)$, and $F(s)$ is given by (10b), shown at the bottom of the page, with Λ_i, Λ_m, and Λ_e denoting the admittivity operators of the cytoplasm, cell membrane, and extracellular medium, respectively.

Amplification of the external field in the membrane at $\theta = 0$ is then

$$G_E(s) = \frac{E_m(s)}{E_e(s)} = \frac{R}{d}F(s). \qquad (11)$$

The basic principle of the method can be illustrated by a block diagram shown in Fig. 3. The external electric field represents the "input" or the "excitation" of the system, $G_E(s)$ plays the role of a transfer function, while the induced transmembrane voltage and membrane field are the "outputs" or the

$$F(s) = \frac{3\Lambda_e[3dR^2\Lambda_i + (3d^2R - d^3)(\Lambda_m - \Lambda_i)]}{2R^3(\Lambda_m + 2\Lambda_e)\left(\Lambda_m + \frac{1}{2}\Lambda_i\right) - 2(R - d)^3(\Lambda_e - \Lambda_m)(\Lambda_i - \Lambda_m)} \qquad (10b)$$

"responses." For any given time course of the external electric field, this method gives the time course of the TMV, as well as of the membrane field.

While the use of this approach in the analysis of transients is described elsewhere [14], this paper focuses on the analysis of membrane fields induced by ac (sinusoidal) fields at different frequencies. With a sinusoidal time course of the external field with frequency $f = \omega/2\pi$, the complex frequency becomes purely imaginary, and the admittivity operators Λ are replaced by the *admittivities*,

$$\lambda^* = \lambda + j\omega\varepsilon \qquad (12)$$

whereby $G_E(s)$ is transformed into $G_E(\omega)$.

III. RESULTS

By inserting (10b) into (11) and replacing Λ_i, Λ_m, and Λ_e by λ_i^*, λ_m^*, and λ_e^*, respectively, one gets (13), shown at the bottom of the page. The limiting values of $G_E(\omega)$ at $\omega \to 0$ and $\omega \to \infty$ are derived in the Appendix, and under physiological conditions they can be approximated by

$$|G_E(0)| \approx \frac{3R}{2d}, \quad \angle G_E(0) = 0° \qquad (14)$$

$$|G_E(\infty)| \approx \frac{3\varepsilon_i\varepsilon_e}{\varepsilon_m(\varepsilon_i + 2\varepsilon_e)}, \quad \angle G_E(\infty) = 0°. \qquad (15)$$

With typical parameter values (see Table I), one gets $|G_E(0)| \approx 3000$ and $|G_E(\infty)| \approx 15$. Thus, the membrane field strength induced at very high frequencies still exceeds the external field strength by more than one order of magnitude.

A stable amplification at high frequencies is not anticipated by the first-order model, as (7) testifies. Also, the first-order model predicts the phase lag to asymptotically approach $-90°$, while according to (15), $E(t)$ and $E_m(t)$ are again close to synchronization at very high frequencies. Absence of the high-frequency plateau in the classical treatment originates from the assumption of purely conductive cytoplasm and extracellular medium; namely, if ε_i and ε_e are set to zero, the amplification given by (15) is easily shown to become zero—the value predicted by (7).

Using the same numerical values as in Fig. 1, Bode plot of $G_E(\omega)$ given by (13) is depicted in Fig. 4 by a solid line, while the one predicted by (5) is drawn in dashed line. The two models agree at low frequencies, but while (5) prognosticates a continuing decrease of magnitude and phase stabilized at $-90°$, (13) exhibits a second breakpoint frequency, where the magnitude stabilizes at the *high-frequency plateau*. Also
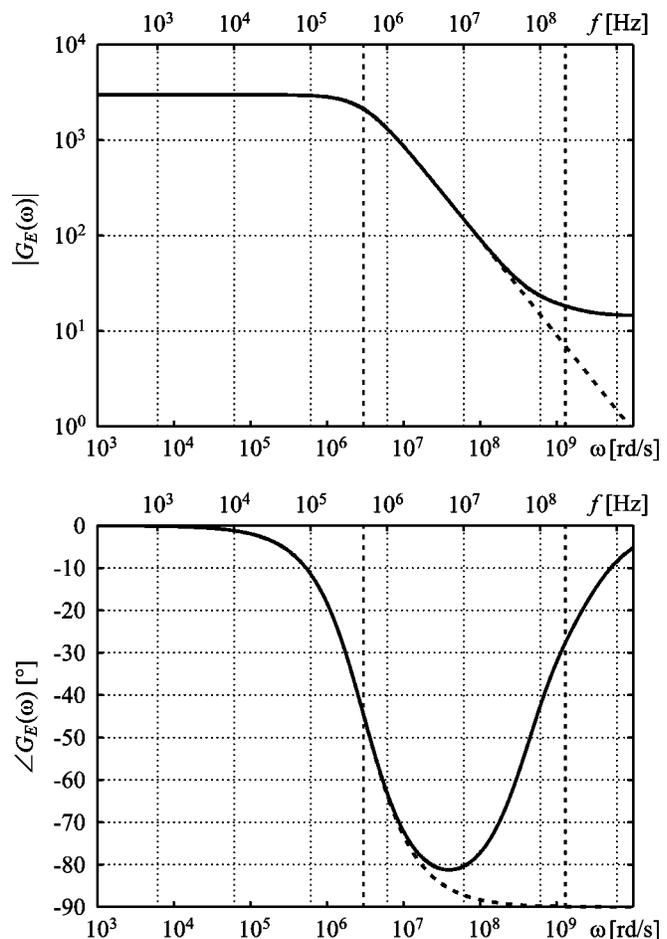

Fig. 4. Bode plot of the amplification of an external ac electric field in the membrane according to the second-order treatment given by (13) (solid line), and the predictions of the first-order model (dashed). The two bold dotted verticals correspond to the first (left) and the second (right) breakpoint frequency: $f_1 = 1/(2\pi\tau_{m1})$ and $f_2 = 1/(2\pi\tau_{m2})$. Parameter values used in the calculation are given in Table I.

due to the second breakpoint frequency, the phase does not approach $-90°$, but reaches a peak level, and then gradually falls back toward zero.

Though (13) allows for analytical derivation of the limiting values, as well as numerical calculation of the whole frequency dependence of G_E, it does not in itself clearly reveal the behavior of $G_E(\omega)$ demonstrated in Fig. 4. Though both the numerator and the denominator of (13) are of second order, making membrane field inducement a *second-order process*, Fig. 4 clearly implies that this process can be approximated as first-order. This is to say that both the numerator and denominator of (13) act approximately as if they were of first order (unlike this, the classical model given by (5) has a first-order denominator, but the numerator is frequency-independent, i.e.,

$$G_E(\omega) = \frac{3\lambda_e^*[3R^3\lambda_i^* + (3dR^2 - d^2R)(\lambda_m^* - \lambda_i^*)]}{2R^3(\lambda_m^* + 2\lambda_e^*)\left(\lambda_m^* + \frac{1}{2}\lambda_i^*\right) - 2(R-d)^3(\lambda_e^* - \lambda_m^*)(\lambda_i^* - \lambda_m^*)} \qquad (13)$$
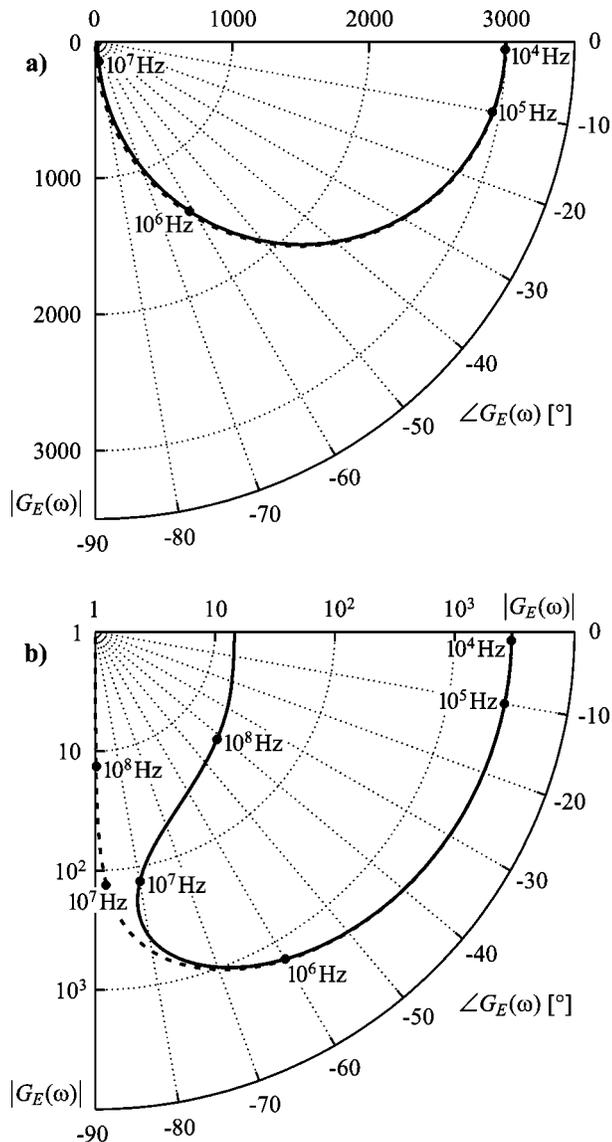
Fig. 5. Nyquist (Cole-Cole) plot of the amplification of an external electric field in the membrane according to the second-order (solid line) and the first-order model (dashed). (a) Linear magnitude scale. (b) Logarithmic magnitude scale. For used parameter values, see Table I and caption of Fig. 4.

of zeroth order). Sections A and B of the Appendix are dedicated to an in-depth analysis and elucidation of this behavior demonstrated by $G_E(\omega)$.

Another customary representation of the frequency dependence is a Nyquist (Cole-Cole) plot, which shows the trajectory of the amplification in the complex plane. Fig. 5 compares the Nyquist plots of $G_E(\omega)$ given by (13) and (5). When a linear magnitude scale is used, the distinctions are hardly visible, thus confirming a good agreement between the two equations [Fig. 5(a)]. With a logarithmic magnitude scale, the differences at higher frequencies are emphasized [Fig. 5(b)].

IV. DISCUSSION

Two principal aims of this section are 1) to discuss the limitations of the presented model and 2) to contemplate on possible

implications of the high-frequency plateau, which is overlooked by the classical first-order model.

A. Limitations of the Model

It has been shown that with intercellular distance several times larger than cell radius, the effect of neighboring cells on induced transmembrane voltage is negligible [16]. All the expressions presented in this paper are therefore valid for a single cell and also for dilute cell suspensions, but they fail to provide a reliable quantitative analysis for tissues, where cells are densely packed. Nevertheless, the qualitative predictions of the second-order model—the second plateau of the membrane field and its synchronization with the external field at high frequencies—also apply to tissues.

While (5) accurately describes membrane field amplification up to ca. 10 MHz, with (13) the upper frequency limit of validity is increased by at least an order of magnitude. As the frequency exceeds several hundreds of megahertz, the finite mobility of molecular dipoles starts to weaken the polarization processes. This shows as a decrease in the permittivities of the materials and a coupled increase in their conductivity, known as dielectric relaxation. For frequencies above 100 MHz, (12) must thus be reformulated to give an *effective admittivity*

$$\lambda^* = \lambda(\omega) + j\omega\varepsilon(\omega) \qquad (16)$$

which has a more intricate dependence upon frequency than (12). By implementing effective admittivities into (13), the description of the field amplification is extended to the frequencies where the dielectric relaxation occurs.

For estimative calculations, dielectric properties of the extracellular medium can be well approximated by those of the physiological NaCl solution at 35°C, for which precise data on dielectric relaxation are available [17]. On the other hand, the established techniques are very difficult to implement on anisotropic materials, and data on relaxation of lipids remain very scarce. Results have been published on dielectric spectroscopy of colloidal suspensions of phospholipid vesicles [18], and more recently of multilamellar bilayers [19]. To our knowledge, no measurements have yet been reported directly on unilamellar lipid bilayers, or cell membranes. An alternative approach is offered by the measurements of lipid headgroup rotation obtained by P-NMR and ^{2}H-NMR [20], [21]. In general, dielectric relaxation of water and aqueous ionic solutions becomes pronounced at GHz frequencies, while the relaxation of bilayer lipids occurs at hundreds of megahertz, thereby setting the upper limit for validity of the presented second-order treatment at approximately 100 MHz.

B. Effects of the High-Frequency Plateau

In the two paragraphs that follow, we shortly discuss possible effects of the high-frequency plateau on two well-known phenomena caused by the exposure to ac electric fields: 1) electric power dissipation, which occurs in every material and is greatly enhanced at high frequencies, and 2) electropermeabilization (electroporation), a field-induced increase of cell membrane permeability and conductivity. Both electric power dissipation and electropermeabilization lead to alterations in the

structure and properties of cellular molecules, thus affecting the cellular functions. The effects of both phenomena can be reversible, with exposed cells recovering from the damage, or irreversible (in general, at larger perturbations), leading to cell death. In the next paragraphs, we consider the relevance of each of the two phenomena at high frequencies.

1) High-Frequency Power Dissipation: Power dissipation P per unit volume of a material is given by [22]

$$P(\omega) = \lambda(\omega) \cdot |E|^2 \tag{17}$$

where E is the strength of the ac electric field with the angular frequency ω, and $\lambda(\omega)$ is the effective conductivity of the material at this angular frequency. Above the relaxation frequency, the effective conductivity of a given material increases significantly, which according to (17) leads to a proportional increase of power dissipation (the effect widely exploited in the microwave ovens). The dielectric relaxation of the lipid bilayer occurs in the 100-MHz range, while in the aqueous media it only becomes expressed above 1 GHz (hence, the use of 2.45 GHz in the microwave ovens). Due to the high-frequency plateau, the membrane field is stable in this frequency range, and this implies that between 100 MHz and 1 GHz, power dissipation in the membrane increases significantly. Due to the small membrane thickness, the elevated power dissipation probably cannot lead to significant temperature increase within the membrane, but it might result in nonthermal effects. The distributed power dissipation at high frequencies is explored in detail in [23].

2) High-Frequency Electropermeabilization: According to the established theory, electro-permeabilization is a nonthermal phenomenon [24], [25]. It only occurs if the transmembrane voltage (and hence the membrane electric field) exceeds a certain threshold value, which according to different authors ranges between 0.250 V and 1 V [26]–[28]. For a cell with $R = 10\,\mu m$, transmembrane voltage of 1 V is induced by an external field of $E \approx 670$ V/cm, provided that the reciprocal of the pulse duration lies within the low-frequency plateau (which is true for the typical pulses used for electropermeabilization, ranging from tens of microseconds to tens of milliseconds). Such a field is generated by applying approximately 67 V to a 1 mm poration cuvette, or by a voltage of 268 V with a 4-mm cuvette. As $G_E(\infty)$ is two orders of magnitude lower than $G_E(0)$, electropermeabilization by nanosecond pulses would demand voltages hundred times larger, and is thus practically unachievable with current technology. Possibility of electropermeabilization occurring accidentally due to the exposure to high-frequency sources such as cellular phones or radio-frequency emitting antennas can thus also be excluded beyond any reasonable doubt.

APPENDIX

A. Exact Formulations of $G_E(\omega)$

By expanding both the numerator and denominator of (13), a rational function is obtained

$$G_E(\omega) = \frac{a_1(j\omega)^2 + a_2 j\omega + a_3}{b_1(j\omega)^2 + b_2 j\omega + b_3} \tag{A1}$$

where

$$\begin{aligned}
a_1 &= 3\varepsilon_i\varepsilon_e(3R^3 - 3dR^2 + d^2R) \\
&\quad + 3\varepsilon_m\varepsilon_e(3dR^2 - d^2R), \tag{A2a}
\end{aligned}$$

$$\begin{aligned}
a_2 &= 3(\lambda_i\varepsilon_e + \lambda_e\varepsilon_i)(3R^3 - 3dR^2 + d^2R) \\
&\quad + 3(\lambda_m\varepsilon_e + \lambda_e\varepsilon_m)(3dR^2 - d^2R) \tag{A2b}
\end{aligned}$$

$$\begin{aligned}
a_3 &= 3\lambda_i\lambda_e(3R^3 - 3dR^2 + d^2R) \\
&\quad + 3\lambda_m\lambda_e(3dR^2 - d^2R) \tag{A2c}
\end{aligned}$$

$$\begin{aligned}
b_1 &= 2R^3(\varepsilon_m + 2\varepsilon_e)\left(\varepsilon_m + \frac{1}{2}\varepsilon_i\right) \\
&\quad + 2(R-d)^3(\varepsilon_m - \varepsilon_e)(\varepsilon_i - \varepsilon_m) \tag{A2d}
\end{aligned}$$

$$\begin{aligned}
b_2 &= 2R^3\left(\lambda_i\left(\frac{1}{2}\varepsilon_m + \varepsilon_e\right) + \lambda_m\left(\frac{1}{2}\varepsilon_i + 2\varepsilon_m + 2\varepsilon_e\right)\right. \\
&\quad \left. + \lambda_e(\varepsilon_i + 2\varepsilon_m)\right) \\
&\quad + 2(R-d)^3(\lambda_i(\varepsilon_m - \varepsilon_e) + \lambda_m(\varepsilon_i - 2\varepsilon_m + \varepsilon_e) \\
&\quad\quad - \lambda_e(\varepsilon_i - \varepsilon_m)) \tag{A2e}
\end{aligned}$$

and

$$\begin{aligned}
b_3 &= 2R^3(\lambda_m + 2\lambda_e)\left(\lambda_m + \frac{1}{2}\lambda_i\right) \\
&\quad + 2(R-d)^3(\lambda_m - \lambda_e)(\lambda_i - \lambda_m). \tag{A2f}
\end{aligned}$$

Both the polynomial in the numerator and the polynomial in the denominator of (A1) are of second order, giving the process of membrane field inducement the second-order nature.

Equation (A1) can be rewritten as

$$G_E(\omega) = K\frac{(1 + j\omega\tau_{m3})(1 + j\omega\tau_{m4})}{(1 + j\omega\tau_{m1})(1 + j\omega\tau_{m2})} \tag{A3}$$

where the constants are given by

$$K = \frac{a_3}{b_3} \tag{A4a}$$

$$\tau_{m1} = \frac{b_2 + \sqrt{b_2^2 - 4b_1b_3}}{2b_3} \tag{A4b}$$

$$\tau_{m2} = \frac{b_2 - \sqrt{b_2^2 - 4b_1b_3}}{2b_3} \tag{A4c}$$

$$\tau_{m3} = \frac{a_2 + \sqrt{a_2^2 - 4a_1a_3}}{2a_3} \tag{A4d}$$

$$\tau_{m4} = \frac{a_2 - \sqrt{a_2^2 - 4a_1a_3}}{2a_3}. \tag{A4e}$$

Alternatively, (A1) can also be reformulated as a sum of partial fractions

$$G_E(\omega) = K_0 + \frac{K_1}{1 + j\omega\tau_{m1}} + \frac{K_2}{1 + j\omega\tau_{m2}} \tag{A5}$$

where

$$K_0 = \frac{a_1}{b_1} \tag{A6a}$$

$$K_1 = \frac{3}{\sqrt{b_2^2 - 4b_1b_3}}\left[\frac{a_3b_1 - a_1b_3}{b_2 - \sqrt{b_2^2 - 4b_1b_3}} - \frac{a_2b_1 - a_1b_2}{2b_1}\right] \tag{A6b}$$

$$K_2 = \frac{3}{\sqrt{b_2^2 - 4b_1b_3}}\left[\frac{a_2b_1 - a_1b_2}{2b_1} - \frac{a_3b_1 - a_1b_3}{b_2 + \sqrt{b_2^2 - 4b_1b_3}}\right] \tag{A6c}$$

and τ_{m1} and τ_{m2} are given by (A4b) and (A4c), respectively.

The first summand in (A5) represents the synchronous (in-phase) part of the response, while the other two are lagging responses, each characterized by a time constant.

B. Simplifications

To elucidate the properties of $G_E(\omega)$ shown in Fig. 4, one has to consider the realistic physiological conditions, where two relations build a basis for simplifications:

- membrane conductivity, λ_m, is more than five orders of magnitude smaller than the conductivities of the cytoplasm, λ_i, and the extracellular medium, λ_e (see Table I); therefore, by disregarding λ_m where it appears in sum with λ_e or λ_i, the obtained result differs from the exact value by several parts in a million.
- membrane thickness, d, is at least three orders of magnitude smaller than cell radius, R; by approximating $(R - d) \approx R$, one commits an error in the range of at most several parts in a thousand.

It should be stressed that with terms that include both conductive and dimensional parameters, the first of the above mentioned relations has to be considered before the second one, as the error committed by the first approximation is far smaller than the one introduced by the second. Furthermore, disregarder of the membrane conductivity often leads to cancellation of additional terms, including the ones that contain parameters R and d, as becomes apparent in the calculation of $G_E(0)$ and $G_E(\infty)$ presented later.

Applying the rules set above to the terms (A2a)–(A2f), one gets

$$a_1 \approx 9R^3 \varepsilon_i \varepsilon_e \tag{A7a}$$

$$a_2 \approx 9R^3 (\lambda_i \varepsilon_e + \lambda_e \varepsilon_i) \tag{A7b}$$

$$a_3 \approx 9R^3 \lambda_i \lambda_e \tag{A7c}$$

$$b_1 \approx 3R^3 \varepsilon_m(\varepsilon_i + 2\varepsilon_e) + 6R^2 d \varepsilon_i \varepsilon_e \tag{A7d}$$

$$b_2 \approx 3R^3 \varepsilon_m(\lambda_i + 2\lambda_e) + 6R^2 d(\lambda_i \varepsilon_e + \lambda_e \varepsilon_i) \tag{A7e}$$

and

$$b_3 \approx 3R^3 \lambda_m(\lambda_i + 2\lambda_e) + 6R^2 d \lambda_i \lambda_e. \tag{A7f}$$

As these expressions are inserted into (A4a)–(A4e), the resulting constants read

$$K \approx \frac{3R}{2d} \tag{A8a}$$

$$\tau_{m1} \approx \frac{\varepsilon_m}{\frac{d}{R}\frac{2\lambda_i \lambda_e}{\lambda_i + 2\lambda_e} + \lambda_m} \tag{A8b}$$

and

$$\tau_{m2} \approx \tau_{m3} \approx \tau_{m4} \approx \frac{\varepsilon_i + 2\varepsilon_e}{\lambda_i + 2\lambda_e}. \tag{A8c}$$

This sheds some light on the behavior of $G_E(\omega)$ shown in Fig. 4. As the three time constants τ_{m2}, τ_{m3}, and τ_{m4} are very close together (with realistic parameter values, the difference between them never exceeds one part in a thousand), they can be approximated as equal. This cancels out two of the multiplicands in (A3), leading to the first-order expression

$$G_E(\omega) \approx \frac{3R}{2d}\left[\frac{1 + j\omega\tau_{m2}}{1 + j\omega\tau_{m1}}\right] \tag{A9}$$

with time constants given by (A8b) and (A8c). Expression (A8b) equals the first-order time constant given by (1), i.e., $\tau_{m1} = \tau_m$, thus confirming once again the validity of the established predictions of low-frequency behavior. The reciprocals of the two time constants of (A9), $(\tau_{m1})^{-1}$ and $(\tau_{m2})^{-1}$, correspond to the two breakpoint frequencies in the Bode plot in Fig. 4.

Equations (A7a)–(A7f) also allow (A6a)–(A6c) to be approximated as

$$K_0 \approx \frac{3\varepsilon_e \varepsilon_i}{\varepsilon_m(\varepsilon_i + 2\varepsilon_e)} \tag{A10a}$$

$$K_1 \approx \frac{3R}{2d} - \frac{3\varepsilon_i \varepsilon_e}{\varepsilon_m(\varepsilon_i + 2\varepsilon_e)} \tag{A10b}$$

and

$$K_2 \approx 0. \tag{A10c}$$

Equation (A10c) reflects the fact that with physiological parameter values, K_2 is more than nine orders of magnitude smaller than both K_0 and K_1, making the second lagging response negligible in any practical context, and validating the approximation of membrane field inducement by

$$G_E(\omega) \approx K_0 + \frac{K_1}{1 + j\omega\tau_{m1}} \tag{A11}$$

with K_0 and K_1 given by (A10a) and (A10b), respectively.

C. Limits $G_E(0)$ and $G_E(\infty)$

The low-frequency limit of $G_E(\omega)$ is obtained by inserting $\omega = 0$ into (13). This leads to (A12), shown at the bottom of the page. Since $\lambda_m \ll \lambda_i, \lambda_e$, we approximate $\lambda_m = 0$. We then obtain an expression which depends only on the geometric parameters of the cell

$$|G_E(0)| \approx \frac{3R}{2d}. \tag{A13}$$

In a similar manner, the limit at $\omega \to \infty$ reads as (A14), shown at the top of the next page. Since no conductivities appear in this expression, simplification is based on the relation $d \ll R$, which we approximate with $d = 0$. This leads to an expression which depends only on the material parameters of the cell

$$|G_E(\infty)| \approx \frac{3\varepsilon_e \varepsilon_i}{\varepsilon_m(\varepsilon_i + 2\varepsilon_e)} \tag{A15}$$

$$|G_E(0)| = \frac{3\lambda_e[3R^3\lambda_i + (3dR^2 - d^2R)(\lambda_m - \lambda_i)]}{2R^3(\lambda_m + 2\lambda_e)\left(\lambda_m + \frac{1}{2}\lambda_i\right) - 1(R - d)^3(\lambda_e - \lambda_m)(\lambda_i - \lambda_m)}, \quad \angle G_E(0) = 0° \tag{A12}$$

$$|G_E(\infty)| = \frac{3\varepsilon_e[3R^3\varepsilon_i + (3dR^3 - d^2R)(\varepsilon_m - \varepsilon_i)]}{2R^3(\varepsilon_m + 2\varepsilon_e)\left(\varepsilon_m + \frac{1}{2}\varepsilon_i\right) - 2(R - d)^3(\varepsilon_e - \varepsilon_m)(\varepsilon_i - \varepsilon_m)}, \quad \angle G_E(\infty) = 0° \quad \text{(A14)}$$

REFERENCES

[1] E. Neumann, M. Schaefer-Ridder, Y. Wang, and P. H. Hofschneider, "Gene transfer into mouse lyoma cells by electroporation in high electric fields," *EMBO J.*, vol. 1, pp. 841–845, 1982.

[2] L. M. Mir, S. Orlowski, J. Belehradek Jr., J. Teissié, M. P. Rols, G. Serša, D. Miklavčič, R. Gilbert, and R. Heller, "Biomedical applications of electric pulses with special emphasis on antitumor electrochemotherapy," *Bioelectrochem. Bioenerg.*, vol. 38, pp. 203–207, 1995.

[3] G. Serša, M. Čemažar, and D. Miklavčič, "Antitumor effectiveness of electrochemotherapy with cis-diamminedichloroplatinum(II) in mice," *Cancer Res.*, vol. 55, pp. 3450–3455, 1995.

[4] Y. Mouneimne, P. F. Tosi, R. Barhoumi, and C. Nicolau, "Electroinsertion of full length recombinant CD4 into red blood cell membrane," *Biochim. Biophys. Acta*, vol. 1027, pp. 53–58, 1990.

[5] S. Raffy and J. Teissié, "Insertion of glycophorin A, a transmembraneous protein, in lipid bilayers can be mediated by electropermeabilization," *Eur. J. Biochem.*, vol. 230, pp. 722–732, 1995.

[6] U. Zimmermann, "Electric field mediated fusion and related electrical phenomena," *Biochim. Biophys. Acta*, vol. 694, pp. 227–277, 1982.

[7] A. E. Sowers, *Cell Fusion*. New York: Plenum, 1987.

[8] K. R. Foster and H. P. Schwan, "Dielectric properties of tissues and biological materials: A critical review," *Crit. Rev. Biomed. Eng.*, vol. 17, pp. 25–104, 1989.

[9] G. Führ, R. Glaser, and R. Hagedorn, "Rotation of dielectrics in a rotating electric high-frequency field: Model experiments and theoretical explanation of the rotation effect of living cells," *Biophys. J.*, vol. 49, pp. 395–402, 1985.

[10] H. A. Pohl, *Dielectrophoresis*, London, U.K.: Cambridge Univ. Press, 1978.

[11] H. P. Schwan, "Electrical properties in tissue and cell suspensions," *Adv. Biol. Med. Phys.*, vol. 5, pp. 147–209, 1957.

[12] H. Pauly and H. P. Schwan, "Über die Impedanz einer Suspension von kugelförmigen Teilchen mit einer Schale," *Z. Naturforsch.*, vol. 14B, pp. 125–131, 1959.

[13] C. Grosse and H. P. Schwan, "Cellular membrane potentials induced by alternating fields," *Biophys. J.*, vol. 63, pp. 1632–1642, 1992.

[14] T. Kotnik, D. Miklavčič, and T. Slivnik, "Time course of transmembrane voltage induced by time-varying electric fields—A method for theoretical analysis and its application," *Bioelectrochem. Bioenerg.*, vol. 45, pp. 3–16, 1998.

[15] T. Kotnik, F. Bobanović, and D. Miklavčič, "Sensitivity of transmembrane voltage induced by applied electric fields—A theoretical analysis," *Bioelectrochem. Bioenerg.*, vol. 43, pp. 285–291, 1997.

[16] R. Susil, D. Šemrov, and D. Miklavčič, "Electric field-induced transmembrane potential depends on cell density and organization," *Electro. Magnetobiol.*, vol. 17, pp. 391–399, 1998.

[17] R. Büchner, G. T. Hefter, and P. M. May, "Dielectric relaxation of aqueous NaCl solutions," *J. Phys. Chem. A*, vol. 103, pp. 1–9, 1999.

[18] R. Pottel, K. D. Göpel, R. Henze, U. Kaatze, and V. Uhlendorf, "The dielectric permittivity spectrum of aqueous colloidal phospholipid solutions between 1 kHz and 60 GHz," *Biophys. Chem.*, vol. 19, pp. 233–244, 1984.

[19] B. Klösgen, C. Reichle, S. Kohlsmann, and K. D. Kramer, "Dielectric spectroscopy as a sensor of membrane headgroup mobility and hydration," *Biophys. J.*, vol. 71, pp. 3251–3260, 1996.

[20] E. J. Dufourc, C. Mayer, J. Stohrer, G. Althoff, and G. Kothe, "Dynamics of phosphate head groups in biomembranes," *Biophys. J.*, vol. 61, pp. 42–57, 1992.

[21] A. S. Ulrich and A. Watts, "Molecular response of the lipid headgroup to bilayer hydration monitored by 2H-NMR," *Biophys. J.*, vol. 66, pp. 1441–1449, 1994.

[22] C. Gabriel, S. Gabriel, E. H. Grant, B. S. J. Halstead, and D. M. P. Mingos, "Dielectric parameters relevant to microwave dielectric heating," *Chem. Soc. Rev.*, vol. 27, pp. 213–223, 1998.

[23] T. Kotnik and D. Miklavčič, "Theoretical evaluation of the distributed power dissipation in biological cells exposed to electric fields," *Bioelectromagnetics*, vol. 21, pp. 385–394, 2000.

[24] T. Y. Tsong, "Electroporation of cell membranes," *Biophys. J.*, vol. 60, pp. 297–306, 1991.

[25] J. C. Weaver and Y. A. Chizmadzhev, "Theory of electroporation: A review," *Bioelectrochem. Bioenerg.*, vol. 41, pp. 135–160, 1996.

[26] R. Benz, F. Beckers, and U. Zimmermann, "Reversible electrical breakdown of lipid bilayer membranes: A charge-pulse relaxation study," *J. Membr. Biol.*, vol. 48, pp. 181–204, 1979.

[27] J. Teissié and M. P. Rols, "An experimental evaluation of the critical potential difference inducing cell membrane electropermeabilization," *Biophys. J.*, vol. 65, pp. 409–413, 1993.

[28] D. Miklavčič, K. Beravs, D. Šemrov, M. Čemažar, F. Demšar, and G. Serša, "The importance of electric field distribution for effective in vivo electroporation of tissues," *Biophys. J.*, vol. 74, pp. 2152–2158, 1998.

[29] R. B. Gennis, *Biomembranes: Molecular Structure and Function*. New York: Springer, 1989.

[30] C. M. Harris and D. B. Kell, "The radio-frequency dielectric properties of yeast cells measured with a rapid, automated, frequency-domain dielectric spectrometer," *Bioelectrochem. Bioenerg.*, vol. 11, pp. 15–28, 1983.

[31] R. Hölzel and I. Lamprecht, "Dielectric properties of yeast cells as determined by electrorotation," *Biochim. Biophys. Acta*, vol. 1104, pp. 195–200, 1992.

[32] P. R. C. Gascoyne, R. Pethig, J. P. H. Burt, and F. F. Becker, "Membrane changes accompanying the induced differentiation of Friend murine erythroleukemia cells studied by dielectrophoresis," *Biochim. Biophys. Acta*, vol. 1146, pp. 119–126, 1993.

[33] F. W. Sunderman, "Measurement of serum total base," *Amer. J. Clin. Path.*, vol. 15, pp. 219–222, 1945.

[34] K. Nörtemann, J. Hilland, and U. Kaatze, "Dielectric properties of aqueous NaCl solutions at microwave frequencies," *J. Phys. Chem. A*, vol. 101, pp. 6864–6869, 1997.

Tadej Kotnik was born in 1972 in Ljubljana, Slovenia. He received the B.S.El.Eng. and the M.S.El.Eng. degrees from the University of Ljubljana, in 1995 and 1998, respectively, and is now preparing his Ph.D. thesis at the University of Paris XI, Paris, France.

He is currently a Researcher at the Laboratory of Biocybernetics at the Faculty of Electrical Engineering of the University of Ljubljana, and part-time at the Laboratory of Physical Chemistry and Pharmacology of Biological Macromolecules (UMR 8532 CNRS) of the Institute Gustave-Roussy, Villejuif, France. His main research interests lie in the fields of membrane electrostatics and electrodynamics, as well as in both theoretical and experimental study of related biophysical phenomena, especially membrane electropermeabilization.

Damijan Miklavčič was born in 1963 in Ljubljana, Slovenia. He received the B.S.El.Eng., the M.S.El.Eng., and the Ph.D. degrees from the University of Ljubljana, in 1987, 1991, and 1993, respectively.

He is currently an Associate Professor and the Head of the Laboratory of Biocybernetics at the Faculty of Electrical Engineering of the University of Ljubljana. His research areas of interest are biomedical engineering and study of the interaction of electromagnetic fields with biological systems. In the last years he has focused on engineering aspects of electropermeabilization as the basis of drug delivery into cells in tumor models *in vitro* and *in vivo*. His research includes biological experimentation, numerical modeling, and hardware development for electrochemotherapy.